Journal of Innovative Technology, Vol. 3, No. 1, pp. 27-33, March 2021
http://doi.org/10.29424/JIT.202103_3(1).0005

Performance of Dye-sensitized Solar Cell Based on AZO/TiO_2 Photoelectrode and RGO@TiO_2/Pt Counter Electrode

Jung-Chuan Chou [1*], Chung-Ming Yang [2], Jun-Xiang Chang [2], Chih-Hsien Lai [3], Yu-Hsun Nien [4], Po-Yu Kuo [5], Yu-Che Lin [2], and Zhen-Rong Yong [6]

ABSTRACT

This study demonstrated a simple fabrication of counter electrode for dye-sensitized solar cell (DSSC). The reduced graphene oxide (RGO) was mixed with titanium dioxide (TiO_2), which was used to improve the adhesion of RGO to platinum (Pt) counter electrodes. In addition, the photoelectrode for DSSC was fabricated using radio frequency (R. F.) sputtering method to deposit the aluminum doped zinc oxide (AZO) film as a barrier layer on TiO_2 layer. The DSSCs combined with RGO@TiO_2 counter electrodes and AZO/TiO_2 photoelectrodes were measured under the effect of different light intensities. Moreover, we adopted the electrochemical impedance spectroscopy (EIS) system to better measure Nyquist plots. Also, the technique of cyclic voltammetry (CV) was used to measure and verify the electrocatalytic activity of RGO@TiO_2 counter electrodes. The EIS and CV showed that the RGO@TiO_2 counter electrodes had high electrocatalytic activity for the reduction of I_3^-.

Keywords: Dye-sensitized solar cell, reduced graphene oxide, titanium dioxide, aluminum doped zinc oxide, electrochemical impedance spectrometer, cyclic voltammetry.

1. INTRODUCTION

Due to population expansion and industrial development, the energy shortage is a very serious issue of our time. Green energy and energy storage are the most popular topics in this century. Solar photovoltaic modules can generate electricity through the sunshine, and it is considered the most valuable in green energy technologies. Therefore, solar energy has been the hottest issue over the last decade, and now solar energy is the fastest-growing industry as well.

Dye-sensitized solar cell (DSSC) is the third generation of the solar cell. DSSCs have many advantages. They are low cost material and are not affected by temperature. Also, the process is easy because it is simple to process this equipment. One of the important components in DSSC is photoelectrodes, which is used to absorb dye and generate the electrons when DSSC operates under the light (Baek and Eo 2017). The photoelectrode of DSSC is usually fabricated with nanoporous materials, such as titanium dioxide (TiO_2) and zinc oxide (ZnO), and porous materials are used to increase the dye adsorption and enhance the light harvest (Chappel and Zaban 2002; Dou *et al.* 2011; Qiu *et al.* 2010). The other important component in DSSC is the Pt counter electrode. The Pt counter electrode is used to collect electron from the external circuit and restores the I^-/I_3^- redox-coupled (Hong *et al.* 2008; Huang *et al.* 2017).

Pt is an excellent conductive and stable material, and yet it is an expensive material. Therefore, Pt have been replaced by many cheaper materials in recent years, such as carbon nanotubes, carbon black and graphene, etc. (Murakami *et al.* 2006; Nam *et al.* 2010; Wang *et al.* 2015). Reduced graphene oxide (RGO) is a kind of carbonaceous material, which can be converted from graphene oxide (GO) through heat treatment (Gao *et al.* 2010). After heat treatment, the electrical conductivity and catalytic activity of RGO are better than those of GO (Ma *et al.* 2014; Tang and Gou 2010). The RGO has been applied in the counter electrode because it exhibits remarkable electrical, optical, and mechanical properties (Wang *et al.* 2014). The research group of Tsai used the RGO and macrocyclic iron (Fe) to synthesize complex hybrid materials and used them in the counter electrodes of DSSCs (Tsai *et al.* 2017). The research group of Wang synthesized PRGO by using annealing treatment, and the PRGO was applied for the counter electrodes of DSSCs (Wang *et al.* 2014).

Aluminum doped zinc oxide (AZO) is a common and low-cost semiconductor material. The AZO has been regarded as a substitute for tin-doped indium oxide (ITO) in recent years, because of the advantages of AZO, such as excellent electrical conductivity and optical transmittance (Minami 2008). In 2010, the research group of Noh (Noh *et al.* 2010) used AZO film to form transparent conductive oxide (TCO) layer and deposited the

---

Manuscript received August 19, 2020; revised September 5, 2020; accepted September 17, 2020.

[1*] Honorary Chair Professor (corresponding author), Department of Electronic Engineering, National Yunlin University of Science and Technology, Douliou, Yunlin, Taiwan 64002, R.O.C. (e-mail: choujc@yuntech.edu.tw).

[2] Student, Department of Electronic Engineering, National Yunlin University of Science and Technology, Douliou, Yunlin, Taiwan 64002, R.O.C.

[3] Professor, Department of Electronic Engineering, National Yunlin University of Science and Technology, Douliou, Yunlin, Taiwan 64002, R.O.C.

[4] Professor, Department of Chemical and Materials Engineering, National Yunlin University of Science and Technology, Douliou, Yunlin, Taiwan 64002, R.O.C.

[5] Associate Professor, Department of Electronic Engineering, National Yunlin University of Science and Technology, Douliou, Yunlin, Taiwan 64002, R.O.C.

[6] Student, Department of Chemical and Materials Engineering, National Yunlin University of Science and Technology, Douliou, Yunlin, Taiwan 64002, R.O.C.

Nb-doped TiO_2 on AZO film for photoelectrode. In 2016, the research group of Chen used the grey relational Taguchi method to find the optimal sputtering parameters of AZO film and used this as a TCO layer (Chen *et al*. 2016). Some research groups also used the AZO film to replace the TiO_2 because the electron affinity and electron injection efficiency of AZO are similar to that of TiO_2 (Kim *et al*. 2014). In 2011, the research group of Yun fabricated the DSSC with AZO nanofiber photoelectrodes prepared by seed layer treatment. The AZO film is commonly used as a transparent conductive oxide film in DSSC, but the AZO film was used as a barrier layer on the TiO_2 layer in this study (Yun and Lim, 2011).

In general, solar cell shows the poor photovoltaic conversion efficiency under indoor light sources, but DSSCs can demonstrate the better photovoltaic conversion efficiency under indoor light sources (Freitag *et al*. 2017). Another advantage of DSSCs is that the DSSCs are not affected by the angle of incident light because the nano TiO_2 photoelectrode has larger specific surface area (Ito *et al*. 2004). The DSSCs have the potential to be combined with flexible substrate and indoor appliances to better become green energy equipment.

In this study, we included the RGO to improve the electrocatalytic activity of Pt counter electrodes, and used the AZO film as a barrier layer on TiO_2 photoelectrodes. The solar simulator was used to measure the photovoltaic parameters of DSSCs. The electrochemical impedance spectroscopy (EIS) system and cyclic voltammetry (CV) measurement were used to investigate the electrocatalytic activity of counter electrodes for DSSCs.

2. EXPERIMENTS

2.1 Materials

The reduced graphene oxide (RGO) powder was purchased from Ruilnog Photoelectric technology Co., LTD, Taiwan. The aluminum doped zinc oxide (AZO) target and platinum (Pt) target were purchased from Ultimate Materials Technology Co. Ltd., Taiwan. The ethanol was purchased from Katayama Chemical, Japan. The titanium dioxide (TiO_2) powders (P25) and Ruthenium-535 (N3) were purchased from UniRegion Bio-Tech, Taiwan. The 1-propyl-2, 3-dimethylimidazolium iodide (DMPII) and acetone were purchased from Tokyo Chemical, Japan. The Triton X-100 was purchased from PRS Panreac, Spain. The 4-Tert-Butylpyridine (TBP), acetylacetone (AcAc), and lithium iodide (LiI) were purchased from Sigma-Aldrich, United States. The 1-Methyl-2-Pyrrolidinone Anhydrosolv (NMP) and potassium hydroxide (KOH) were purchased from Echo Chemical Co., Taiwan. The iodine puriss (I_2) was purchased from Riedel-de Haën, Germany.

2.2 Fabrication of AZO/TiO_2 Phtoelectrode of the DSSC

The fluorine doped tin oxide (FTO) glass substrate was cleaned by acetone, ethanol and deionized (D. I.) water with ultrasonic cleaner for 30 min, respectively. the cleaned FTO glass was heated in the oven at 120°C for 30 min, and the excess water was also removed by nitrogen. The TiO_2 layer had double structures in this photoelectrode. The TiO_2 colloid for adsorption layer, which was composed of 3 g TiO_2 powders, 6 mL D. I. water, 0.05 mL of acetylaceton (AcAc) and 0.15 mL of Trition X-100. For scattering layer, the 1 g TiO_2 powders, 0.4 mL ethanol and 4 mL D. I. water were put into dark bottles. The TiO_2 colloids for adsorption layer and scattering layer were stirred for 24 h by a magnetic stirrer at room temperature. First of all, the TiO_2 colloid for adsorption layer was deposited onto the cleaned FTO glass by spin-coating method and deposited the TiO_2 colloid for scattering layer by doctor-blade method on the TiO_2 adsorption layer. The double TiO_2 photoelectrodes were annealed at 450°C for 30 min in air ambient. After the annealing treatment, the AZO barrier layer was deposited on TiO_2 double layer by the radio frequency sputtering method. Subsequently, the AZO/TiO_2 photoelectrodes were annealed and sintered at 450°C for 30 min in air ambient again. Finally, AZO/TiO_2 photoelectrodes were immersed in 3×10^{-4} M N3 dye.

2.3 Fabrication of RGO@TiO_2/Pt Counter Electrode of DSSC

First of all, 5 mL D. I. water, 5 mL NMP and 0.05 g RGO powder were mixed, and the RGO solution was formed. Next, the 0.6 g TiO_2 powder, 2 mL D. I. water, 0.02 mL AcAc and 0.04 mL Trition X-100 were used to blend the RGO@TiO_2 colloid. The platinum (Pt) counter electrode of DSSC was deposited by radio frequency sputtering method and the deposition time was 6 min. The RGO@TiO_2 film was deposited on Pt counter electrode by spin-coating method. The electrolyte was composed of 0.6 M 1-propyl-2, 3-dimethylimidazolium iodide (DMPII), 0.5 M lithium iodide (LiI), 0.05 M iodine and 0.5 M 4-tert-butylpyridine (TBP) in 15 mL 3-methoxypropionitrile (MPN). The AZO/TiO_2 photoelectrode and Pt counter electrode were assembled into a typical sandwich-type cell. Then, electrolytes were added to the middle between the photoelectrodes and RGO@TiO_2/Pt counter electrodes. Figure 1 shows the schematic device of a DSSC using the AZO/TiO_2 photoelectrodes and RGO@TiO_2/Pt counter electrodes.

2.4 Measurement System

The solar simulator (MFS-PV-Basic-HMT, Taiwan), the light intensity of which was 100 mW/cm^2, was used to measure the photovoltaic parameters of the DSSCs. In order to confirm whether the DSSCs could achieve the better photovoltaic conversion efficiency under the low light intensity environment, we used the different filters to not only control the light intensities but also measure photovoltaic parameters of the DSSCs. The Nyquist plot of DSSC was analyzed by electrochemical impedance spectroscopy (BioLogic SP-150, France) with frequency from 50 mHz to 1 MHz. The cyclic voltammetry (BioLogic SP-150, France) of RGO@TiO_2 counter electrodes for DSSC was investigated with a scan rate of 120 mV/s. Field emission scanning electron microscope (FE-SEM, Hitachi S4800-I, Japan) was used to the investigate the morphology of RGO@TiO_2 counter electrodes.

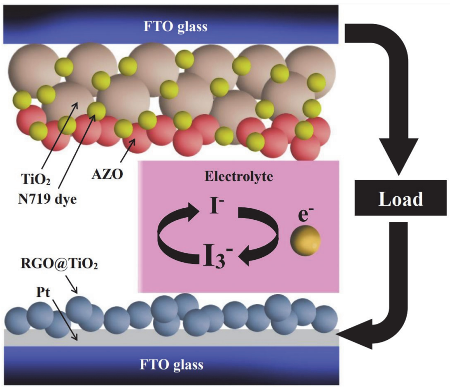

Fig. 1 The schematic of AZO/TiO_2 photoelectrodes and RGO@TiO_2/Pt counter electrode DSSCs.

3. RESULTS AND DISCUSSION

We employed a simple fabrication to form the RGO@TiO_2 film and deposited this on Pt layer in this study. The surface morphology and structure of RGO@TiO_2 counter electrodes was investigated by field emission scanning electron microscope (FE-SEM). Figure 2 illustrates the FE-SEM images of RGO@TiO_2 counter electrodes. The top view for RGO@TiO_2 is given in Fig. 2 (a). Clearly, the RGO nanosheet was surrounded by TiO_2 nanoparticles, as presented in Fig. 2 (a). The purpose of adding TiO_2 to the RGO solution was to use the TiO_2 to better improve the adsorption of RGO and Pt. Therefore, the TiO_2 nanoparticles and RGO nanosheet could be observed in Fig. 2 (a). Figure 1 (b) depicts the cross section of RGO@TiO_2 counter electrodes with a thickness of 18.6 μm to 18.8 μm.

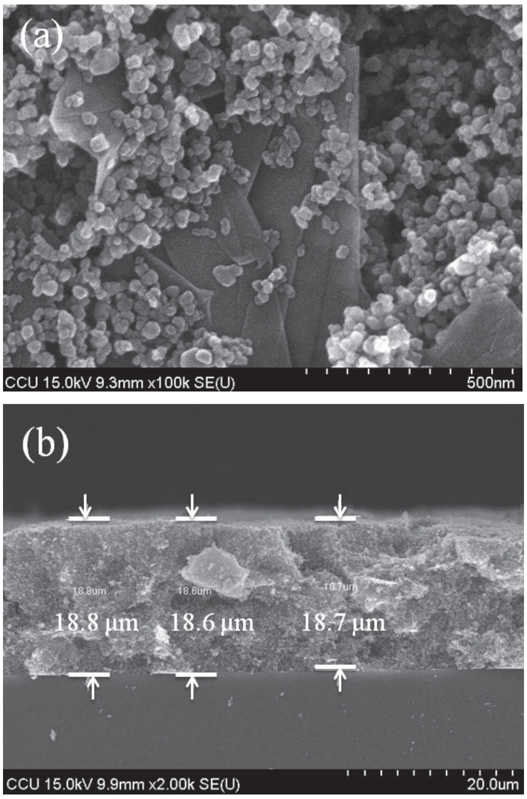

Fig. 2 The FE-SEM images for (a) the top view of RGO@TiO_2 counter electrodes and (b) the cross section of RGO@TiO_2 counter electrodes.

The photovoltaic parameters of DSSCs with different photoelectrodes and different counter electrodes are exhibited in Table 1. From Table 1, the DSSCs based on AZO/TiO_2 photoelectrodes and RGO@TiO_2 counter electrodes achieved the open circuit voltage (V_{OC}), short circuit current density (J_{SC}), fill factor (F. F.) and optimal photovoltaic conversion efficiency (η). The order of their values were 0.69 V, 11.15 mA/cm2, 59.24% and 4.52%, respectively. In comparison with pure TiO_2 photoelectrodes, the photoelectrodes exhibited the better short circuit current density and photovoltaic conversion efficiency after sputtering AZO barrier layer on TiO_2 layer, for the AZO barrier could effectively reduce the electron recombination between the interface of TiO_2 and electrolytes. The attenuation of fill factor after sputtering AZO barrier layer took place because of the decrease of impedance matching in DSSC. The AZO is a kind of metallic oxide material, we mixed the metallic oxide with DSSC, and this resulted in the decrease of impedance matching. After adding the RGO to modify the Pt counter electrodes, the short circuit current density and photovoltaic conversion efficiency were improved from 10.52 mA/cm^2 to 11.15 mA/cm^2 and from 4.01% to 4.52%. The increases of short circuit current density and photovoltaic conversion efficiency were attributed to RGO, which improved the electrocatalytic capacity for reducing the I^-/I_3^- redox-coupled. Figure 3 shows the current density - voltage (J - V) curves of DSSCs with different photoelectrodes and different counter electrodes. The results showed that the short circuit current density of DSSC based on AZO photoelectrode and RGO@TiO_2 counter electrode was higher than that of the other DSSCs under the same conditions in this study. Table 1 summarizes the photovoltaic parameters comparison of counter electrodes of RGO and GO structures. In the Ref. (Zhao *et al.* 2019), the RGO films were prepared by thermal conversion. In the Ref. (Sarker *et al.* 2017), the RGO counter electrode was prepared by doctor-blading method for Pt-free counter electrode of DSSC, and as to the DSSC based on RGO counter electrode, the photovoltaic conversion efficiency was achieved 4.04%. In the Ref. (Qiu *et al.* 2014), the RGO counter electrode was prepared by drop casting method and followed by heat treatment, and the photovoltaic conversion efficiency of DSSC based on RGO counter electrode was 2.62%. In the Ref. (Bajpai *et al.* 2011), the composite material counter electrode of DSSC was fabricated by graphene (G) and Pt nanoparticles, the photovoltaic conversion efficiency was achieved 2.91%. In the Ref. (Jang *et al.* 2012), RGO film were fabricated by simple and fast thermal treatment of solution processed GO. The RGO was treated at 350°C and used as a counter electrode of DSSC, and the DSSC showed the photovoltaic conversion efficiency of 3.60%.

Table 1 The photovoltaic parameters of DSSCs with different photoelectrodes and different counter electrodes.

Photoelectrode	Counter electrode	V_{OC} (V)	J_{SC} (mA/cm^2)	F. F. (%)	η (%)	References
TiO_2	Pt	0.68	05.52	65.98	2.51	In this study
AZO/TiO_2	Pt	0.72	10.52	52.85	4.01	In this study
AZO/TiO_2	RGO@TiO_2/Pt	0.69	11.15	59.24	4.52	In this study
TiO_2	$Ni_{12}P_5$/RGO	0.70	19.55	60.00	8.19	(Wang *et al.* 2020)
TiO_2	RGO	0.67	12.93	73.00	6.35	(Zhao *et al.* 2019)
TiO_2	RGO	0.69	09.89	58.73	4.04	(Sarker *et al.* 2017)
TiO_2	RGO	0.68	09.47	40.50	2.62	(Qiu *et al.* 2014)
TiO_2	G-Pt	0.74	06.67	59.00	2.91	(Bajpai *et al.* 2011)
TiO_2	GO 350°C	0.66	16.35	33.33	3.60	(Jang *et al.* 2012)

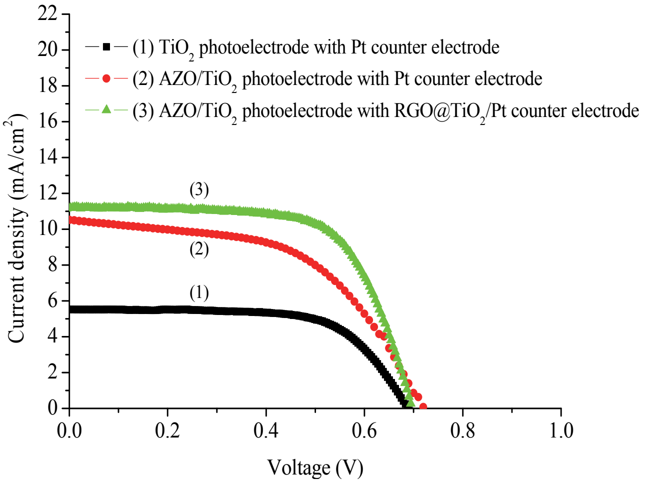

Fig. 3 **The current density - voltage curves of DSSCs with different photoelectrodes and different counter electrodes.**

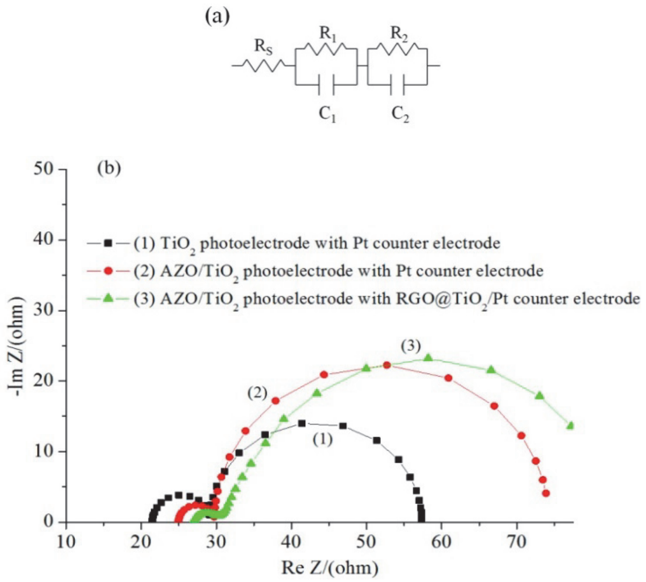

Fig. 4 **(a) The equivalent circuit model of DSSCs and (b) the Nyquist plots of DSSCs with different photoelectrodes and different counter electrodes.**

The analysis of interface impedance corresponding DSSCs were usually investigated by the electrochemical impedance spectroscopy (EIS) measurement. Therefore, we capitalized on the EIS system to analyze the interface impedance of DSSCs. The DSSCs were measured under the dark environment, andthe scanning frequency was from 1 MHZ to 50 mHZ. Figure 4 (a) is the equivalent circuit model of DSSCs. In general, the RS represents series resistance between the FTO glass and wires. The R_1 represents the charge transfer impedance between electrolyte and counter electrode. The R_2 represents electron recombination impedance between the interfaces of TiO_2/dye/electrolyte (Longo *et al.* 2003). The C_1 and C_2 in the equivalent circuit model of DSSCs could be ignored because the C_1 and C_2 were large capacitances when the DSSCs were operated under the direct-current condition (Chou *et al.* 2017; Seo *et al.* 2012) Figure. 4 (b) shows the Nyquist plots of DSSCs with different photoelectrodes and different counter electrodes. Table 2 lists the impedance Rs, R1, R2 of different photoelectrode and counter electrode, respectively. Comparing to the conventional Pt electrodes, the R_1 value of RGO@TiO_2/Pt counter electrodes was reduced significantly. This might have suggested an enhancement in the catalytic activity of the redox process. This was also confirmed by the CV results. In addition, compared to other counter electrodes, the counter electrodes with RGO@TiO_2 were found to have a more obvious impedance drop (7.63ohm to 3.92ohm).

Besides, the cyclic voltammetry measurement is considered as an important experiment to be conducted in order to better verify the electrocatalytic ability of the counter electrodes. Figure 5 shows the cyclic voltammetry (CV) curves of Pt counter electrodes and RGO@TiO_2/Pt counter electrodes. The scan rate of CV measurement was 120 mV/s. The oxidation peak and reduction peak are given in Fig. 5. The peak at the positive current density is oxidation peak and corresponds the equation (1); the peak at negative current density is the reduction peak and corresponds to the equation (2). The RGO@TiO_2/Pt CE showed a commendable reduction and an oxidation current density. On the other hand, Pt showed a similar reduction and a lesser oxidation current density. The peak-to-peak separation (E_{PP}) is an important parameter to compare the electrocatalytic ability of counter electrodes for DSSCs. In general, a lower E_{PP} stands for a better electrocatalytic ability (Yao *et al.* 2013). From Fig. 5, the EPP of RGO@TiO_2 counter electrodes were similar to the Pt counter electrodes. Both were approximately 0.56 V. Moreover, the higher reduction current density represents a faster rate for I_3^- reduction (Wang *et al.* 2013). The peak current density of the RGO@TiO_2/Pt counter electrodes was 2.62 mA/cm^{-2}, which was larger than the Pt counter electrodes (1.26 mA/cm^2). Compared with the Pt counter electrodes, the peak current density of the RGO@TiO_2/Pt counter electrodes was increased by 2.07 times, and the Epp values were similar. This part of the results demonstrates that the RGO@TiO_2/Pt counter electrode possessed higher electrocatalytic activity towards the reduction of I_3^- than the Pt counter electrodes did.

Table 2 **The electrochemical impedance parameters of DSSCs with different photoelectrodes and different counter electrodes.**

Photoelecrode	Counter electrode	R_S (ohm)	R_1 (ohm)	R_2 (ohm)	References
TiO_2	Pt	21.50	7.63	28.23	In this study
AZO/TiO_2	Pt	25.03	4.78	44.52	In this study
AZO/TiO_2	RGO@TiO_2/Pt	27.31	3.92	47.09	In this study
TiO_2	Pt	12.13	0.83	N/A	(Wang *et al.* 2020)
TiO_2	$Ni_{12}P_5$/RGO	11.56	0.79	N/A	(Wang *et al.* 2020)
TiO_2	Ni_2P/RGO	13.03	1.65	N/A	(Wang *et al.* 2020)

$$3I^- \rightarrow I3^- + 2e^- \quad (1)$$

$$I3^- + 2e^- \rightarrow 3I^- \quad (2)$$

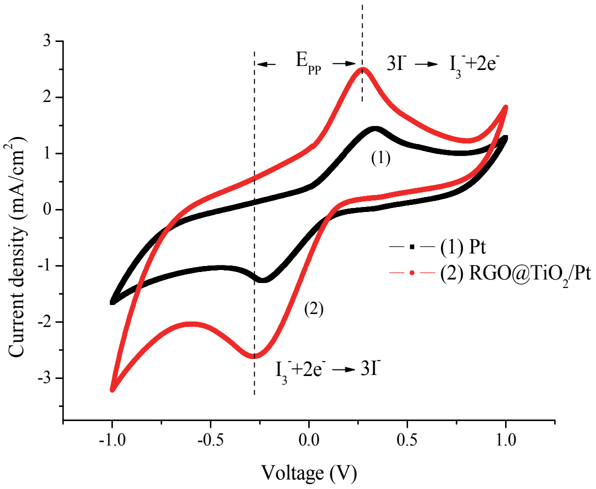

Fig. 5 The cyclic voltammetry curves of Pt counter electrodes and RGO@TiO$_2$/Pt counter electrodes.

To confirm whether the DSSCs could operate under the lower light environment, we not only used different filters to produce different light intensities but also measured the photovoltaic parameters of DSSCs under the different light intensities by a solar simulator. The light intensities were 100 mW/cm^2, 80 mW/cm^2, 50 mW/cm^2, 30 mW/cm^2, 10 mW/cm^2, respectively. Table 3 presents the photovoltaic parameters of DSSCs with AZO/TiO$_2$ photoelectrodes and RGO@TiO$_2$/Pt counter electrodes under different light intensities. As can be seen from Table 3, the photovoltaic conversion efficiency was increased significantly when the light intensity dropped. This was especially obvious when the light intensity was reduced to 30 mW/cm^2, and so a photovoltaic conversion efficiency of 5.41% was obtained for the DSSCs. The decrease noticed in the short circuit current density was due to the decrease of the excited electrons under the low light intensities. The open circuit voltage was decreased when the DSSCs were operated under the lower light intensities. This phenomenon was attributed to the fewer excited electrons injected into TiO$_2$, and so enabled the Fermi level of TiO$_2$ to be decreased (Lan *et al.* 2012; Salvador *et al.* 2005). Also, the increment of fill factor under low light intensity was attributed to less diffusion overpotential (Zhai *et al.* 2016). We also used the T5 fluorescent light and different filters to measure the lower light intensities. The light intensities were 1.4 mW/cm^2, 0.9 mW/cm^2, 0.6 mW/cm^2, 0.2 mW/cm^2, respectively. According to Table 3, the DSSCs achieved the photovoltaic conversion efficiency of 6.45% under the T5 fluorescent light. Especially, when the DSSCs were operated under 0.6 mW/cm^2, the DSSCs exhibited 11.73% photovoltaic conversion efficiency. The photovoltaic conversion efficiency of DSSCs under T5 fluorescent light was higher than that observed under the solar simulator, and this resulted from the fact thatthe ruthenium dye had a stronger spectral response to the T5 spectral distribution (Zhai *et al.* 2016). Another reason for the increased photovoltaic conversion efficiency under the low light intensity is that the reduced electron recombination took place (Kim *et al.* 2015). Figure 6 shows the Nyquist plots of DSSCs with AZO/TiO$_2$ photoelectrodes and RGO@TiO$_2$/Pt counter electrodes under the different T5 fluorescent light intensities. Figure 7 shows the enlarged view of Fig. 6. Clearly, a significant increase was found in the second semicircle and the electron recombination impedance. It represented the lower electron recombination at the TiO$_2$/electrolyte interface, and the lower electron recombination was due to the decreased excited electrons (Kim *et al.* 2015). In addition, the fill factors increased under the low light intensities, and this was attributed to the reduction of electron recombination, as suggested by Kim *et al.* (2015). Therefore, the increase in the photovoltaic conversion efficiency under the low light intensity is mainly attributed to the increment of fill factors and the reduction of electron recombination.

Table 3 The photovoltaic parameters of DSSC with AZO/TiO$_2$ photoelectrodes and RGO@TiO$_2$/Pt counter electrodes under different light intensities.

Light intensity (mW/cm^2)	V_{OC} (V)	J_{SC} (mA/cm^2)	F. F. (%)	η (%)
100	0.69	11.15	59.24	4.52
80	0.68	8.75	62.47	4.68
50	0.67	5.69	64.13	4.89
30	0.66	3.75	66.05	5.41
10	0.64	1.25	66.88	5.33
1.7 mW/cm^2 (T5 fluorescent light)	0.63	0.26	67.54	6.45
1.4	0.61	0.24	68.72	7.02
0.9	0.59	0.19	70.19	8.57
0.6	0.58	0.17	71.64	11.73
0.2	0.56	0.13	70.89	8.26

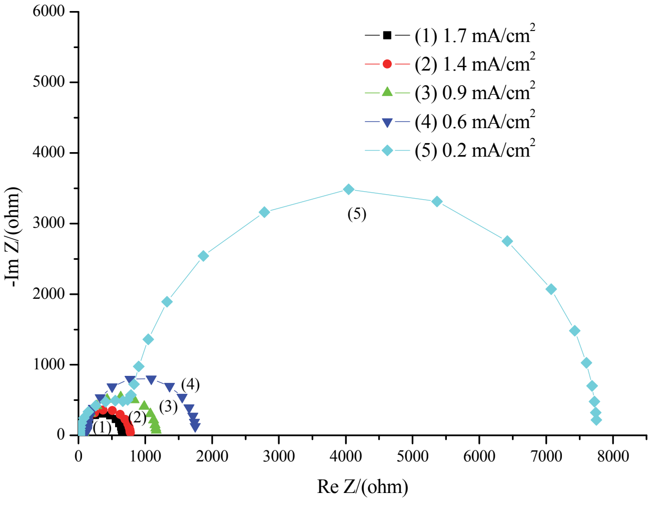

Fig. 6 The Nyquist plots of DSSC with AZO/TiO$_2$ photoelectrodse and RGO@TiO$_2$/Pt counter electrodes under the different T5 fluorescent light intensities.

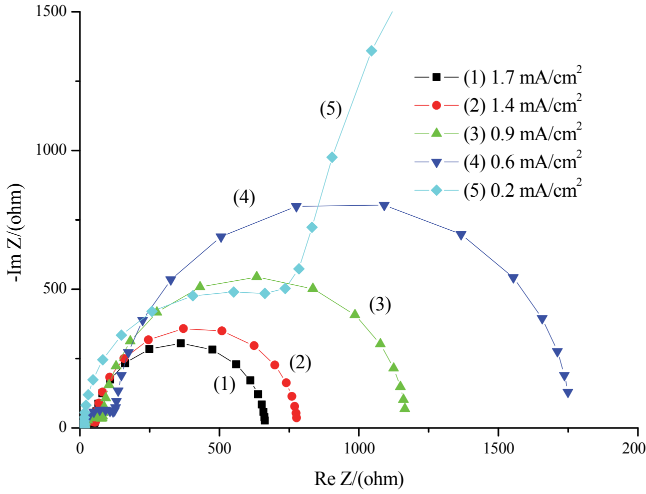

Fig. 7 The enlarged view of DSSC with AZO/TiO_2 photoelectrode and RGO@TiO_2/Pt counter electrode under the different T5 fluorescent light intensities.

4. CONCLUSION

In summary, this study set out to determine a simple fabrication of RGO electrodes for DSSCs. We mixed the TiO_2 with RGO colloid to provide the tight adhesion between the RGO film and the Pt layer. The RGO improved the superior electrocatalytic capacity needed for reducing the I^-/I_3^- redox-coupled. The DSSCs with AZO/TiO_2 photoelectrodes and RGO@TiO_2/Pt counter electrodes achieved the open circuit voltage of 0.69 V, short circuit current density of 11.15 mA/cm^2, fill factor of 59.24% and photovoltaic conversion efficiency of 4.52%, respectively. The EIS and CV results showed the excellent electrocatalytic ability of RGO@TiO_2/Pt counter electrodes. In this study, the DSSCs were also operated under low light intensities. When the light intensity was reduced to 30 mW/cm^2, the DSSCs achieved a photovoltaic conversion efficiency of 5.41%. The increment of photovoltaic conversion efficiency was attributed to both the increased fill factor and the reduced electron recombination. In order to confirm whether the DSSCs could operate under the indoor light sources, we also measured the DSSCs under the T5 fluorescent light (1.7 mW/cm^2). For the DSSCs, a e photovoltaic conversion efficiency of 6.45% was obtained under T5 fluorescent lights. The DSSCs especially achieved a photovoltaic conversion efficiency of 11.73% under the 0.6 mW/cm^2. According to the experiment results, the DSSCs have great potential to be applied to indoor equipment in the future.

REFERENCES

Baek, H.R. and Eo, I.S. (2017). “Electrochemical properties of TiO_2-metal oxide composites for dye-sensitized solar cell.” *Current Applied Physics*, **17**(6), 854-857. doi:10.1016/j.cap.2017.03.014

Bajpai, R., Roy, S., Kumar, P., Bajpai, P., Kulshrestha, N., Rafiee, J., and Misra, D.S. (2011). “Graphene supported platinum nanoparticle counter-electrode for enhanced performance of dye-sensitized solar cells.” *Acs Applied Materials & Interfaces*, **3**(10), 3884-3889. doi:10.1021/am200721x

Chappel, S. and Zaban, A. (2002). “Nanoporous SnO_2 electrodes for dye-sensitized solar cells: improved cell performance by the synthesis of 18 nm SnO_2 colloids.” *Solar Energy Materials and Solar Cells*, **71**(2), 141-152. doi:10.1016/s0927-0248(01)00050-2

Chen, D.Y., Kao, J.Y., Hsu, C.Y., and Tsai, C.H. (2016). “The effect of AZO and compact TiO_2 films on the performance of dye-sensitized solar cells.” *Journal of Electroanalytical Chemistry*, **766**, 1-7. doi:10.1016/j.jelechem.2016.01.012

Chou, J.C., You, P.H., Liao, Y.H., Lai, C.H., Chu, C.M., Lin, Y.J., and Nien, Y.H. (2017). “Fabrication and photovoltaic properties of dye-sensitized solar cells based on graphene-TiO_2 composite photoelectrode with ZnO nanowires.” *Ieee Transactions on Semiconductor Manufacturing*, **30**(4), 531-538. doi:10.1109/tsm.2017.2747121

Dou, X.C., Sabba, D., Mathews, N., Wong, L.H., Lam, Y.M., and Mhaisalkar, S. (2011). “Hydrothermal synthesis of high electron mobility Zn-doped SnO_2 nanoflowers as photoanode material for efficient dye-sensitized solar cells.” *Chemistry of Materials*, **23**(17), 3938-3945. doi:10.1021/cm201366z

Freitag, M., Teuscher, J., Saygili, Y., Zhang, X., Giordano, F., Liska, P., and Hagfeldt, A. (2017). “Dye-sensitized solar cells for efficient power generation under ambient lighting.” *Nature Photonics*, **11**(6), 372-378. doi:10.1038/nphoton.2017.60

Gao, X. F., Jang, J., and Nagase, S. (2010). “Hydrazine and thermal reduction of graphene oxide: reaction mechanisms, product structures, and reaction design.” *Journal of Physical Chemistry C*, **114**(2), 832-842. doi:10.1021/jp909284g

Hong, W.J., Xu, Y.X., Lu, G.W., Li, C., and Shi, G.Q. (2008). “Transparent graphene/PEDOT-PSS composite films as counter electrodes of dye-sensitized solar cells.” *Electrochemistry Communications*, **10**(10), 1555-1558. doi:10.1016/j.elecom.2008.08.007

Huang, N., Li, G.W., Xia, Z.F., Zheng, F., Huang, H., Li, W.J., and Sun, X.H. (2017). “Solution-processed relatively pure MoS_2 nanoparticles in-situ grown on graphite paper as an efficient FTO-free counter electrode for dye-sensitized solar cells.” *Electrochimica Acta*, **235**, 182-190. doi:10.1016/j.electacta.2017.02.111

Ito, S., Matsui, H., Okada, K., Kusano, S., Kitamura, T., Wada, Y., and Yanagida, S. (2004). “Calibration of solar simulator for evaluation of dye-sensitized solar cells.” *Solar Energy Materials and Solar Cells*, **82**(3), 421-429. doi:10.1016/j.solmat.2004.01.030

Jang, H.S., Yun, J.M., Kim, D.Y., Park, D.W., Na, S.I., and Kim, S.S. (2012). “Moderately reduced graphene oxide as transparent counter electrodes for dye-sensitized solar cells.” *Electrochimica Acta*, **81**, 301-307. doi:10.1016/j.electacta.2012.07.021

Kim, H.H., Park, C., Choi, W., Cho, S., Moon, B., and Son, D.I. (2014). “Low-temperature-fabricated ZnO, AZO, and SnO_2 nanoparticle-based dye-sensitized solar cells.” *Journal of the Korean Physical Society*, **65**(9), 1315-1319. doi:10.3938/jkps.65.1315

Kim, J.H., Moon, K.J., Kim, J.M., Lee, D., and Kim, S.H. (2015). “Effects of various light-intensity and temperature environments on the photovoltaic performance of dye-sensitized solar cells.” *Solar Energy*, **113**, 251-257. doi:10.1016/j.solener.2015.01.012

Lan, J.L., Wei, T.C., Peng, S.P., Wan, C.C., and Cao, G.Z. (2012). “Effects of iodine content in the electrolyte on the charge transfer and power conversion efficiency of dye-sensitized solar cells under low light intensities.” *Journal of Physical Chemistry C*, **116**(49), 25727-25733. doi:10.1021/jp309872n

Longo, C., Freitas, J., and De Paoli, M.A. (2003). “Performance and stability of TiO_2/dye solar cells assembled with flexible electrodes and a polymer electrolyte.” *Journal of Photochemistry and Photobiology a-Chemistry*, **159**(1), 33-39. doi:10.1016/s1010-6030(03)00106-0

Ma, J., Zhou, L., Li, C., Yang, J.H., Meng, T., Zhou, H.M., and Chen, J.H. (2014). “Surfactant-free synthesis of graphene-functionalized carbon nanotube film as a catalytic counter electrode in dye-sensitized solar cells.” *Journal of Power Sources*, **247**, 999-1004. doi:10.1016/j.jpowsour.2013.08.145

Minami, T. (2008). “Present status of transparent conducting oxide ing oxide thin-film development for Indium-Tin-Oxide (ITO) substitutes.” *Thin Solid Films*, **516**(17), 5822-5828. doi:10.1016/j.tsf.2007.10.063

Murakami, T.N., Ito, S., Wang, Q., Nazeeruddin, M.K., Bessho, T., Cesar, I., and Gratzel, M. (2006). “Highly efficient dye-sensitized solar cells based on carbon black counter electrodes.” *Journal of the Electrochemical Society*, **153**(12), A2255-A2261. doi:10.1149/1.2358087

Nam, J.G., Park, Y.J., Kim, B.S., and Lee, J.S. (2010). “Enhancement of the efficiency of dye-sensitized solar cell by utilizing carbon nanotube counter electrode.” *Scripta Materialia*, **62**(3), 148-150. doi:10.1016/j.scriptamat.2009.10.008

Noh, J.H., Han, H.S., Lee, S., Kim, D.H., Park, J.H., Park, S., and Hong, K.S. (2010). “A newly designed Nb-doped TiO_2/Al-doped ZnO transparent conducting oxide multi layer for electrochemical photoenergy conversion devices.” *Journal of Physical Chemistry C*, **114**(32), 13867-13871. doi:10.1021/jp104247t

Qiu, L.F., Zhang, H.Y., Wang, W.G., Chen, Y.M., and Wang, R. (2014). “Effects of hydrazine hydrate treatment on the performance of reduced graphene oxide film as counter electrode in dye-sensitized solar cells.” *Applied Surface Science*, **319**, 339-343. doi:10.1016/j.apsusc.2014.07.133

Qiu, Y.C., Chen, W., and Yang, S.H. (2010). “Double-Layered Photoanodes from Variable-Size Anatase TiO_2 Nanospindles: A Candidate for High-Efficiency Dye-Sensitized Solar Cells.” *Angewandte Chemie-International Edition*, **49**(21), 3675-3679. doi:10.1002/anie.200906933

Salvador, P., Hidalgo, M.G., Zaban, A., and Bisquert, J. (2005). “Illumination intensity dependence of the photovoltage in nanostructured TiO_2 dye-sensitized solar cells.” *Journal of Physical Chemistry B*, **109**(33), 15915-15926. doi:10.1021/jp051515l

Sarker, S., Lee, K.S., Seo, H.W., Jin, Y.K., and Kim, D.M. (2017). “Reduced graphene oxide for Pt-free counter electrodes of dye-sensitized solar cells.” *Solar Energy*, **158**, 42-48. doi:10.1016/j.solener.2017.09.029

Seo, H., Son, M.K., Kim, J.K., Choi, J., Choi, S., Kim, S.K., and Kim, H.J. (2012). Analysis of current loss from a series-parallel combination of dye-sensitized solar cells using electrochemical impedance spectroscopy.” *Photonics and Nanostructures-Fundamentals and Applications*, **10**(4), 568-574. doi:10.1016/j.photonics.2012.04.011

Tang, Y. and Gou, J.H. (2010). “Synergistic effect on electrical conductivity of few-layer graphene/multi-walled carbon nanotube paper.” *Materials Letters*, **64**(22), 2513-2516. doi:10.1016/j.matlet.2010.08.035

Tsai, C.H., Huang, W.C., Wang, W.S., Shih, C.J., Chi, W.F., Hu, Y.C., and Yu, Y.H. (2017). “Reduced graphene oxide/macrocyclic iron complex hybrid materials as counter electrodes for dye-sensitized solar cells.” *Journal of Colloid and Interface Science*, **495**, 111-121. doi:10.1016/j.jcis.2017.02.002

Wang, G.Q., Xing, W., and Zhuo, S.P. (2013). “Nitrogen-doped graphene as low-cost counter electrode for high-efficiency dye-sensitized solar cells.” *Electrochimica Acta*, **92**, 269-275. doi:10.1016/j.electacta.2013.01.034

Wang, G.Q., Zhang, J., Kuang, S., and Zhuo, S.P. (2015). “Nitrogen-doped porous carbon prepared by a facile soft-templating process as low-cost counter electrode for High-performance dye-sensitized solar cells.” *Materials Science in Semiconductor Processing*, **38**, 234-239. doi:10.1016/j.mssp.2015.04.025

Wang, S., Xie, Y., Shi, K., Zhou, W., Xing, Z., Pan, K., and Cabot, A. (2020). “Monodispersed Nickel Phosphide Nanocrystals in Situ Grown on Reduced Graphene Oxide with Controllable Size and Composition as a Counter Electrode for Dye-Sensitized Solar Cells.” *ACS Sustainable Chemistry & Engineering*, **15**(8), 5920-5926. doi:10.1021/acssuschemeng.0c00005

Wang, Z.G., Li, P.J., Chen, Y.F., He, J.R., Liu, J.B., Zhang, W.L., and Li, Y.R. (2014). “Phosphorus-doped reduced graphene oxide as an electrocatalyst counter electrode in dye-sensitized solar cells.” *Journal of Power Sources*, **263**, 246-251. doi:10.1016/j.jpowsour.2014.03.118

Yao, R.Y., Zhou, Z.J., Hou, Z.L., Wang, X., Zhou, W.H., and Wu, S.X. (2013). “Surfactant-Free $CuInS_2$ Nanocrystals: An Alternative Counter-Electrode Material for Dye-Sensitized Solar Cells.” *Acs Applied Materials & Interfaces*, **5**(8), 3143-3148. doi:10.1021/am400031w

Yun, S.N. and Lim, S. (2011). “Improved conversion efficiency in dye-sensitized solar cells based on electrospun Al-doped ZnO nanofiber electrodes prepared by seed layer treatment.” *Journal of Solid State Chemistry*, **184**(2), 273-279. doi:10.1016/j.jssc.2010.11.024

Zhai, P., Lee, H., Huang, Y.T., Wei, T.C., and Feng, S.P. (2016). “Study on the blocking effect of a quantum-dot TiO_2 compact layer in dye-sensitized solar cells with ionic liquid electrolyte under low-intensity illumination.” *Journal of Power Sources*, **329**, 502-509. doi:10.1016/j.jpowsour.2016.08.118

Zhao, G., C. Feng, H. Cheng, Y. Li and Z.-S. Wang (2019). “In situ thermal conversion of graphene oxide films to reduced graphene oxide films for efficient dye-sensitized solar cells.” *Materials Research Bulletin*, **120**, doi:10.1016/j.materresbull.2019.110609.